

05.3;08.2

Growth mechanism of monolayer on the top facet of Ga-catalyzed GaAs and GaP nanowires

© A.A. Koryakin¹, Yu.A. Ereemeev², S.V. Fedina³, V.V. Fedorov³

¹ St. Petersburg State University, St. Petersburg, Russia

² Institute of Problems of Mechanical Engineering, Russian Academy of Sciences, St. Petersburg, Russia

³ Alferov Federal State Budgetary Institution of Higher Education and Science Saint Petersburg National Research Academic University of the Russian Academy of Sciences, St. Petersburg, Russia

E-mail: koryakinaa@spbau.ru

Received September 2, 2021

Revised November 10, 2021

Accepted November 10, 2021

The growth mechanism of monolayer on the top facet of Ga-catalyzed GaAs and GaP nanowires is investigated. Within the framework of a theoretical model, the maximal monolayer coverage due to the material in the catalyst droplet, the nanowire growth rate and the content of group V atoms in the droplet are found depending on the growth conditions. The estimates of the phosphorus re-evaporation coefficient from neighboring nanowires and substrate are obtained by comparing the theoretical and experimental growth rate of Ga-catalyzed GaP nanowires.

Keywords: III-V nanowires, vapor-liquid-solid growth mechanism, nucleation

DOI: 10.21883/TPL.2022.02.53583.19011

The recent progress in SEM (scanning electron microscopy) *in situ* studies of the vapor–liquid–solid growth of III–V nanowires (NWs) made it possible to examine the process of growth of the top NW face under a catalyst particle in real time [1–5]. This facilitated the publication of a series of theoretical papers focused on the examination of morphology of the catalyst–NW interface [1–4] and mechanisms of monolayer growth on the top NW face [5–9]. It was found that a complete cycle of monolayer formation may either include an incubation period or be a continuous process [6]. In the former case, the NW growth rate is limited by the nucleation of two-dimensional islets at the catalyst–NW interface. In the latter case, the process is governed by the barrier-free mechanism of step formation. It was also found that the morphology of the catalyst–NW interface also affects the monolayer formation mechanism. The aim of the present study is to examine the regimes of monolayer growth in the process of formation of Ga-catalyzed GaAs and GaP NWs (self-catalyzed VLS growth by molecular-beam epitaxy, MBE). According to [6,8,10], the growth rate of the top NW face is limited by nucleation in this case, and, owing to the low solubility of arsenic and phosphorus in gallium, two regimes of monolayer growth may be observed. If the difference between the maximum number of group V atoms in a droplet (N_V) after the nucleation of a new monolayer and the equilibrium number of group V atoms (N_{Veq}) is greater than the number of group V atoms in the monolayer (N_{ML}), the monolayer grows in the „fast regime“ limited by the diffusion of group V atoms in the droplet. In the contrary case (i.e., when difference $N_V - N_{Veq}$ is smaller than N_{ML}), the monolayer first forms in the fast regime at the expense of material in droplet to a coverage equal approximately

to $\theta_{max} = (N_V - N_{Veq})/N_{ML}$ [6,9]. The „slow regime“ of growth then comes into play: the monolayer growth rate is limited by the transfer of group V atoms to the droplet from the gas phase. This regime is observed at small NW radii and/or a low flux of group V atoms. These two scenarios are implemented if the catalyst–NW interface contains only one III–V crystal face (i.e., if the top NW face is not faceted).

Let us use the model of self-catalyzed VLS growth of III–V NWs proposed in [8] to examine the regimes of monolayer growth. The monolayer growth is simulated in two stages. At the first stage, the process of nucleation of an islet on the surface of a filled monolayer is simulated within the classical nucleation theory. The supersaturation growth time is estimated with the material balance equation for group V atoms in the droplet taken into account. At the second stage, the lateral monolayer growth is simulated, and the material balance equation and the equation for the monolayer growth rate are solved simultaneously.

Figure 1 presents the results of simulation of the growth of GaAs NWs with a sphalerite structure in the [111] direction at different values of the total flux density of group V atoms to the droplet (j_V^{tot}), the NW radius (R_0), and the growth temperature (T). The following value of the interfacial energy of the islet boundary obtained in [8] was used in calculations: $\gamma = 0.394 \text{ J} \cdot \text{m}^{-2}$. The contact angle of the droplet and the angle of incidence of the arsenic flux were $\beta = 125^\circ$ and $\alpha_V = 35^\circ$ [11]. The temperature dependence of the coefficient of diffusion of arsenic in gallium was taken from [12]: $D_V = D_{V0} \exp(-E_V/k_B T)$, where $E_V = 0.7 \text{ eV}$, $D_{V0} = 1.59 \cdot 10^{-5} \text{ m}^2 \cdot \text{s}^{-1}$, and k_B is the Boltzmann constant. The fitting coefficient for the islet growth rate is $r_0 = h/\pi$ [8] (h is the monolayer height). The slow growth regime (without faceting of the top NW face)

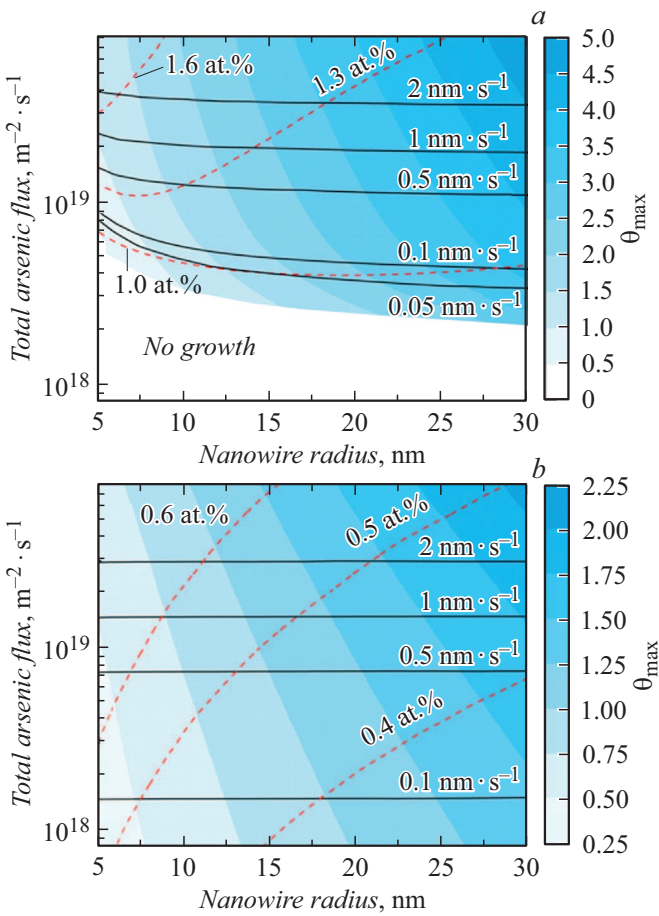


Figure 1. Dependences of θ_{\max} , the GaAs NW growth rate (solid curves), and the molar fraction of arsenic in a droplet (dashed curves) on the arsenic flux and the NW radius at a growth temperature of 600 (a) and 500°C (b).

is established in the region where $\theta_{\max} = (N_V - N_{Veq})/N_{ML}$ is lower than unity. Note that a reduced concentration of group V atoms in the droplet may induce faceting due to the dissolution of the top NW face [4]. The region with $\theta_{\max} < 1$ grows at lower temperatures, since the solubility of group V particles in gallium decreases. The concentration of group V particles in the droplet and, consequently, the θ_{\max} value increase with increasing flux j_V^{tot} . It can be demonstrated via dimensional analysis [6,9] that θ_{\max} depends on the NW radius as $\theta_{\max} \propto (C_V(R_0) - C_{Veq}(T))R_0$, where C_V and C_{Veq} are the maximum and the equilibrium molar fractions of group V particles in the droplet. Since C_V depends only weakly on R_0 (if radius R_0 is not too small), the dependence of θ_{\max} on R_0 for simple estimates may be approximated with a linear function. This agrees well with the results of simulation. At small R_0 values, the desorption flux from the droplet increases due to the dimensional effect, and the concentration of group V atoms decreases drastically as a result [6,11]. In the region of high values of j_V^{tot} and R_0 , molar fraction C_V decreases with increasing R_0 [8,11]. The NW growth rate is then weakly dependent on R_0 , since

the influence of the desorption flux is also weak. This, in turn, indicates that characteristic nucleation time τ_N also depends weakly on R_0 . With formula $\tau_N = 1/\pi R_0^2 I$, where (I is the nucleation intensity) taken into account, we find that the values of I and, consequently, C_V should decrease with increasing R_0 . At high growth temperatures and/or low fluxes j_V^{tot} , the NW growth is virtually nonexistent in a certain region. The white area in Fig. 1, a is such a region with an NW growth rate below $0.005 \text{ nm} \cdot \text{s}^{-1}$. The total flux of group V particles from the gas phase to the droplet in this region is approximately equal to the flux of desorption of group V particles from the droplet: $j_V^{tot} S_V = k_V C_V^2 S_d$, where S_V is the effective area normal to the flux of group V particles intercepted by the droplet; S_d is the droplet surface area; and k_V is the desorption coefficient that depends on C_V , R_0 , and T . The equality of fluxes defines the shape of isocurves $C_V = \text{const}$ in this region.

Total flux density j_V^{tot} of group V atoms to the droplet is expressed in terms of the beam equivalent pressure (BEP) of group V particles in the following way [8,11]: $j_V^{tot} = (1 + \varepsilon_V)\eta p_V$, where p_V is the BEP of group V particles; ε_V is the coefficient of re-evaporation of group V particles from the substrate and neighboring NWs; η is the conversion coefficient defined as $\eta = j_V^{dir}/p_V$ [13]; and j_V^{dir} is the near-substrate density of the direct flux of group V atoms. The value of ε_V determined within models [8,11] by comparing the experimental [13] and theoretical NW growth rates was close to 3. The value of $\eta = 2.3 \cdot 10^{24} \text{ m}^{-2} \cdot \text{s}^{-1} \cdot \text{Torr}^{-1}$ was used for As_4 molecules in [8,11]. However, the η value depends on the configuration of the MBE setup and the calibration of the pressure gage [13]. For example, the conversion coefficient for the As_4 flux in experiments performed in [14] was $1.28 \cdot 10^{24} \text{ m}^{-2} \cdot \text{s}^{-1} \cdot \text{Torr}^{-1}$. The absolute value of the flux of group V atoms was determined by finding the flux at which the regime of growth of planar GaAs [14] and GaP [15] layers switches from Ga-limited growth to V-limited growth. It follows from the comparison of experimental [14] and simulated NW growth rates (at $\gamma = 0.394 \text{ J} \cdot \text{m}^{-2}$) that the coefficient of re-evaporation of arsenic particles is approximately equal to 7. The GaAs and GaP NW growth conditions are detailed in the table.

Figure 2 presents the results of simulation of the growth of GaP NWs with a sphalerite structure in the [111] direction. The interfacial energy for GaP islets used to plot these dependences was $\gamma = 0.47 \text{ J} \cdot \text{m}^{-2}$. This value was determined based on the estimated ratio of surface energies of GaP and GaAs crystals (approximately 1.2 [16]) and the interfacial energy for GaAs islets [8]. Simulation were performed with $\beta = 120^\circ$, $\alpha_V = 30^\circ$, and the phosphorus diffusion coefficient determined in [12]: $E_V = 1.69 \text{ eV}$, $D_{V0} = 4.36 \cdot 10^{-2} \text{ m}^2 \cdot \text{s}^{-1}$. Note that phosphorus atoms are assumed to diffuse in the present study. However, the question of type of phosphorus particles diffusing in liquid gallium requires further study. The dependences of θ_{\max} , C_V , and the NW growth rate on the growth conditions for GaAs and GaP systems agree qualitatively in shape. The

Dependence of re-evaporation coefficient ε_V on the conditions of growth of GaAs and GaP nanowires [14,15] (t is the growth time and V is the rate of axial growth)

$T, ^\circ\text{C}$	t, min	$V, \text{nm} \cdot \text{s}^{-1}$	R_0, nm	$\beta, ^\circ$	$\text{BEP}_{\text{Ga}}, \text{Torr}$	$\text{BEP}_V, \text{Torr}$	$\alpha_V, ^\circ$	ε_V
GaAs								
570	10	0.89	51	~ 120	$1.25 \cdot 10^{-7}$	$1.5 \cdot 10^{-6}$	30	7.0
600	30	1.69	41	~ 120	$1.25 \cdot 10^{-7}$	$3.0 \cdot 10^{-6}$	30	7.2
GaP								
610	60	0.80	104	~ 122	$1.6 \cdot 10^{-7}$	$1.92 \cdot 10^{-6}$	30	5.8
610	60	1.98	81	~ 122	$1.6 \cdot 10^{-7}$	$2.88 \cdot 10^{-6}$	30	7.2
630	60	2.54	42	~ 122	$1.6 \cdot 10^{-7}$	$3.84 \cdot 10^{-6}$	30	11.1

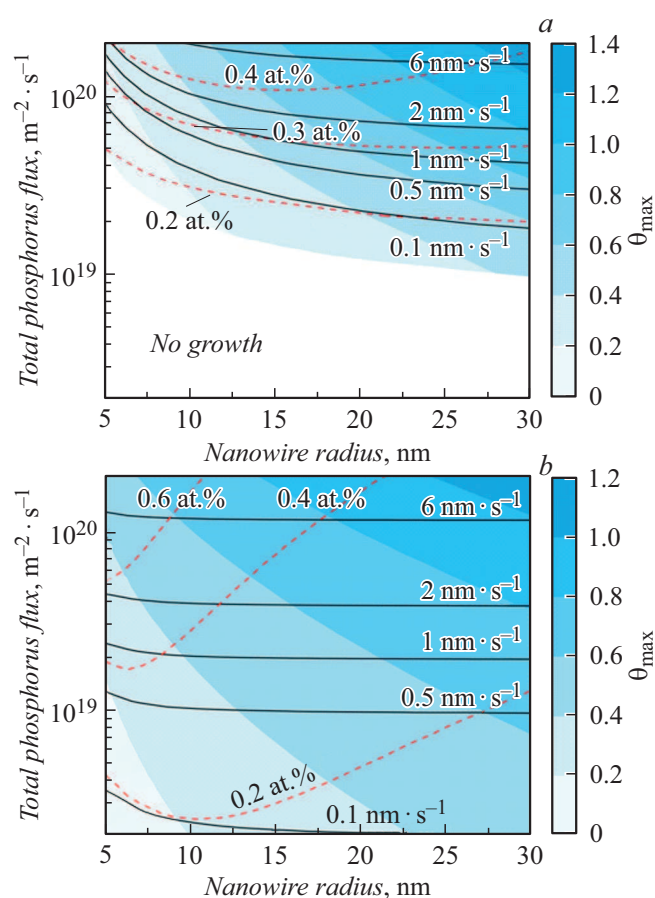


Figure 2. Dependences of θ_{\max} , the GaP NW growth rate (solid curves), and the molar fraction of phosphorus in a droplet (dashed curves) on the phosphorus flux and the NW radius at a growth temperature of 600 (a) and 500°C (b).

boundary of the region with no NW growth in the GaP system is shifted toward higher fluxes, since the desorption flux of phosphorus (P_2) is higher than the desorption flux of arsenic (As_2). This difference in desorption fluxes also explains why the GaP NW growth rate is lower than that for GaAs NWs (at equal values of j_V^{eff}). At the same time, the molar fraction of phosphorus in the gallium catalyst is several times lower than the molar fraction of arsenic in

GaAs NW growth. Therefore, the region of existence of the slow monolayer growth regime ($\theta_{\max} < 1$) is considerably larger.

The experimental data on the growth rate of Ga-catalyzed GaP NWs [15] were compared to the simulated data (see the table) to determine the phosphorus re-evaporation coefficient. The MBE growth on NWs in [15] was performed on Si(111) substrates at a temperature of 610–630°C. The BEP conversion coefficient for P_2 molecules was $\eta = 2.7 \cdot 10^{24} \text{m}^{-2} \cdot \text{s}^{-1} \cdot \text{Torr}^{-1}$. The calculated phosphorus re-evaporation coefficient in GaP NW growth falls within the range of $\varepsilon_V = 6$ –11. The large spread of ε_V is associated with the spread of values of the NW surface density.

Thus, the growth regimes of a monolayer of Ga-catalyzed GaP and GaAs NWs were studied. The obtained dependences of the maximum monolayer coverage and the NW growth rate may be used to optimize the process of VLS NW growth in SEM *in situ* studies.

Funding

The research was carried out as part of project No. 19-72-30004 of the Russian Science Foundation.

Conflict of interest

The authors declare that they have no conflict of interest.

References

- [1] C.-Y. Wen, J. Tersoff, K. Hillerich, M.C. Reuter, J.H. Park, S. Kodambaka, E.A. Stach, F.M. Ross, *Phys. Rev. Lett.*, **107** (2), 025503 (2011). DOI: 10.1103/PhysRevLett.107.025503
- [2] D. Jacobsson, F. Panciera, J. Tersoff, M.C. Reuter, S. Lehmann, S. Hofmann, K.A. Dick, F.M. Ross, *Nature*, **531** (7594), 317 (2016). DOI: 10.1038/nature17148
- [3] J.-C. Harmand, G. Patriarche, F. Glas, F. Panciera, I. Florea, J.-L. Maurice, L. Travers, Y. Ollivier, *Phys. Rev. Lett.*, **121** (16), 166101 (2018). DOI: 10.1103/PhysRevLett.121.166101
- [4] F. Panciera, Z. Baraissov, G. Patriarche, V.G. Dubrovskii, F. Glas, L. Travers, U. Mirsaidov, J.-C. Harmand, *Nano Lett.*, **20** (3), 1669 (2020). DOI: 10.1021/acs.nanolett.9b04808

- [5] C.B. Maliakkal, E.K. Mårtensson, M.U. Tornberg, D. Jacobs-son, A.R. Persson, J. Johansson, L.R. Wallenberg, K.A. Dick, *ACS Nano*, **14** (4), 3868 (2020). DOI: 10.1021/acsnano.9b09816
- [6] F. Glas, V.G. Dubrovskii, *Phys. Rev. Mater.*, **4** (8), 083401 (2020). DOI: 10.1103/PhysRevMaterials.4.083401
- [7] V.G. Dubrovskii, A.S. Sokolovskii, I.V. Shtrom, *Tech. Phys. Lett.*, **46** (9), 889 (2020). DOI: 10.1134/S1063785020090187.
- [8] A.A. Koryakin, S.A. Kukushkin, *Phys. Status Solidi B*, **258** (6), 2000604 (2021). DOI: 10.1002/pssb.202000604
- [9] V.G. Dubrovskii, *Tech. Phys. Lett.*, **46** (4), 357 (2020). DOI: 10.1134/S1063785020040203.
- [10] V.G. Dubrovskii, *Cryst. Growth Des.*, **17** (5), 2589 (2017). DOI: 10.1021/acs.cgd.7b00124
- [11] F. Glas, M.R. Ramdani, G. Patriarche, J.-C. Harmand, *Phys. Rev. B*, **88** (19), 195304 (2013). DOI: 10.1103/PhysRevB.88.195304
- [12] V.A. Gorokhov, T.T. Dedegkaev, Y.L. Ilyin, V.A. Moshnikov, A.S. Petrov, Y.M. Sosov, D.A. Yaskov, *Cryst. Res. Technol.*, **19** (11), 1465 (1984). DOI: 10.1002/crat.2170191112
- [13] M.R. Ramdani, J.C. Harmand, F. Glas, G. Patriarche, L. Travers, *Cryst. Growth Des.*, **13** (1), 91 (2013). DOI: 10.1021/cg301167g
- [14] A.D. Bolshakov, V.V. Fedorov, N.V. Sibirev, M.V. Fetisova, E.I. Moiseev, N.V. Kryzhanovskaya, O.Y. Koval, E.V. Ubyivovk, A.M. Mozharov, G.E. Cirlin, I.S. Mukhin, *Phys. Status Solidi (RRL)*, **13** (11), 1900350 (2019). DOI: 10.1002/pssr.201900350
- [15] V.V. Fedorov, Y. Berdnikov, N.V. Sibirev, A.D. Bolshakov, S.V. Fedina, G.A. Sapunov, L.N. Dvoretckaia, G. Cirlin, D.A. Kirilenko, M. Tchernycheva, I.S. Mukhin, *Nanomaterials*, **11** (8), 1949 (2021). DOI: 10.3390/nano11081949
- [16] S. Mirbt, N. Moll, K. Cho, J.D. Joannopoulos, *Phys. Rev. B*, **60** (19), 13283 (1999). DOI: 10.1103/PhysRevB.60.13283